Annealing of defects created by electron irradiation in bismuth

1989 J. Phys.: Condens. Matter 1 4535

(http://iopscience.iop.org/0953-8984/1/28/005)

J. Phys.: Condens. Matter 1 (1989) 4535–4542. Printed in the UK

Annealing of defects created by electron irradiation in bismuth

P Bois and F Beuneu
Laboratoire des Solides Irradiés (Commissariat à l'Energie Atomique), Ecole Polytechnique, 91128 Palaiseau Cédex, France

Received 15 July 1988, in final form 15 December 1988

Abstract. Pure Bi and Bi-based dilute alloys (doped with Te or Sn) were submitted to isochronal anneals after electron irradiation at an energy ranging from 1 to 2.5 MeV. The resistivity, and in a few cases the magnetoresistance and Hall resistivity, were monitored during these experiments. For 1 MeV irradiations the annealing curves are ideally simple; the whole damage anneals in one single stage near 40 K. For higher energies, or for very high doses at 1 MeV, other additional stages are seen. The alloys exhibit stages at the same temperatures, but the amplitudes vary with the dopant concentration.

1. Introduction

The transport properties of the semimetal Bi when irradiated by electrons [1] were studied in two previous papers. In the first paper [2], we paid attention to the determination of the displacement threshold energy, a measurement which must be considered as a preliminary for all subsequent irradiation studies. We determined a threshold energy near 13 eV for Bi. (The value found enables us to compute the cross sections for a given electron energy. From these cross sections, we know the concentration of defects for a given dose. We also obtain an indication on their nature: primary defects or complexes.) Moreover the behaviour of a Bi–Te dilute alloy sample led us to the conclusion that the mean defect charge depends on the irradiation energy and that Frenkel pairs are donors whereas defect complexes are probably of acceptor type. In the second paper [3], these ideas were confirmed by more direct measurements of the charge of the defects during irradiation via magnetotransport experiments; the donor defect linked to the Frenkel pair was shown to be ionised in all circumstances; the more complicated defects created at high electronic energy (above 1.2 MeV) are of acceptor type and are linked in the density of states to a virtual bound state situated slightly below the pure Bi (intrinsic) Fermi level.

In the present paper, we shall give a complementary account of the experiments described in [3], where attention was focused on defect production. Here we pay attention to isochronal anneals performed on Bi and Bi-based dilute alloys (doped with Sn or Te) after electron irradiation at different doses and at different electron energies: 1, 1.5 and 2.5 MeV. There are a few accounts on a similar subject in the literature: annealing after quenching [4], after fast neutron irradiation [5–7], after electron irradiation [6, 8]. One must also mention the work reported in [9] in which positron annihilation experiments were performed on electron-irradiated samples.

0953-8984/89/284535 + 08 $02.50

Table 1. Characteristics of the samples. The temperature corresponds both to the irradiation temperature and to the reference temperature during the isochronal anneals. The energy and maximum dose of irradiation are also given, together with the impurity concentration for alloys, estimated by the method in [3].

Sample	T (K)	E (MeV)	Dose (dpa)	c (at.ppm)	Comment
Bi–A	4	1 2.5	4.5×10^{-5} 1.8×10^{-3}	0	Bi IV in [3]
Bi–B	20	1	7×10^{-5}	0	
Bi–C	20	2.5	7.5×10^{-3}	0	
Bi–D	20	1.5 2.5	5×10^{-3} 6.3×10^{-3}	0	Orientation z
Bi–E	20	1	2.6×10^{-3}	0	
Bi–Te-A	20	2.5	1×10^{-2}	71	BiTe I in [3]
Bi–Sn-A	20	2.5	1×10^{-2}	45	
Bi–Sn-B	20	2.5	7.5×10^{-3}	150	
Bi–Sn-C	4	2.5	2.5×10^{-3}	210	BiSn VI in [3]

The experimental details are given in § 2. Section 3 gives an account of the experiments concerning the pure Bi samples and a discussion of the salient features of the results. In § 4 the results obtained for the dilute alloys are described.

2. Experimental details

The major part of the present set of experiments is common with those described in [3] so that the experimental procedure is only quickly summarised here. The samples are single-crystal rectangular slabs (typical size, 1 mm × 5 mm × 0.1 mm) such that the normal to the slab is the trigonal axis z whereas the long side is parallel to the binary axis x. There is one exception, with a normal parallel to x axis and a long side parallel to z axis: sample Bi-D, see table 1. In the majority of the experiments, performed at 20 K, the resistivity was the only parameter measured, whereas in the remaining experiments, performed at 4 K, the magnetoresistance and Hall effect curves up to 1.5 T were recorded. The electron irradiations were performed with our Van de Graaff electron accelerator, the energy of which can be varied from 0.5 to 2.5 MeV. The samples were immersed in the cryogenic coolant (liquid H or He).

The samples were submitted to isochronal anneals of 10 min for a series of increasing temperatures. The sample holder was raised above the cryogenic fluid level in a pre-heated oven. During the anneal the temperature of the sample holder was monitored via a Cu–constantan thermocouple. Between anneals the samples were cooled and the transport measurements made. Table 1 describes the samples studied in the present paper; the temperature and energy of irradiation are given together with the concentration of dopant (in atomic parts per million) for the dilute alloys.

3. Pure bismuth

3.1. 1 and 2.5 MeV irradiations: annealing results

In figure 1, we present typical annealing curves obtained for pure Bi samples after electron irradiations either at 1 MeV or at 2.5 MeV and performed at 4 or 20 K. The

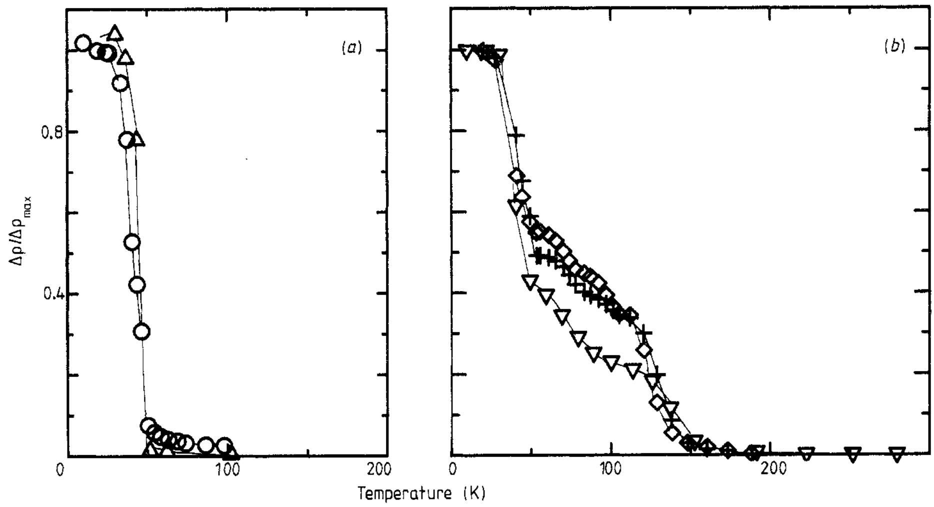

Figure 1. Isochronal annealing of resistivity after (*a*) 1 MeV or (*b*) 2.5 MeV irradiations for pure Bi samples: △, ▽, sample Bi–A; ○, sample Bi–B; ◇, sample Bi–C; +, sample Bi–D. The data are displayed in reduced units as mentioned in the text (§ 3.1). The samples are described in table 1.

total irradiation doses received by the samples are indicated in table 1; the values are expressed in displacements per atom (dpa) and are deduced from the cross section values as mentioned in § 1. All the annealing curves presented in this paper display the relevant parameter (here the increment of electrical resistivity) in reduced units; the ratio of the increment to the initial increment is plotted against temperature, so that the ordinate axis is graduated from 0 to 1. In some cases (see figures 1, 3 and 4), for some low values of the annealing temperature we obtained an increase in the resistivity, which corresponds in our reduced units to values larger than unity. The most striking feature of figure 1 lies in the very simple shape of the 1 MeV curves; the resistivity increment anneals completely in one single stage near 40 K. The magnetotransport experiments on sample Bi-A, analysed with the procedure described in [3], confirm this point by showing that the carrier concentration and the mobilities follow separately the same single-stage behaviour. The 2.5 MeV curves are more complicated; the 40 K stage is again present but total recovery is no longer reached at this stage and several other stages are present at higher temperatures, the main one being situated around 140 K. In figure 2 we show the results of the detailed analysis of magnetotransport experiments performed on the pure Bi sample irradiated at 2.5 MeV and at 4 K, whose behaviour for resistivity is displayed in figure 1; we present the annealing curves of the net carrier imbalance $N - P$ (i.e. the electron concentration minus the hole concentration) and of the inverse $1/\bar{\mu}$ of the electron mobility. The stages are qualitatively the same as in figure 1; however, the 40 K stage appears to have a higher amplitude than for the simple resistivity behaviour.

3.2. Discussion

Here we try to draw come conclusions on the types of defect annealing which occurs in the different stages of our annealing curves. Some help comes from earlier work.

(i) In our preceding papers, we showed through the discussion of threshold energy measurements [2] and resistivity production curves [3] that the nature of irradiation

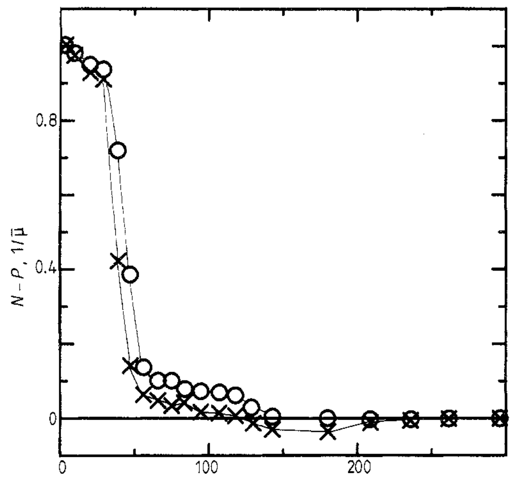

Figure 2. Isochronal annealing of $N-P$ (○) and $1/\bar{\mu}$ (×) after 2.5 MeV irradiation for sample Bi–A.

defects is different; defect agglomerates at 2.5 MeV add up to simple Frenkel pairs obtained at 1 MeV.

(ii) In [4] the quenching of pure Bi and Bi–Te dilute alloys from temperatures near the melting point to liquid-helium temperature was reported. The resistivity increment was determined after subsequent annealing. No recovery at 40 K was observed as the first stage seen was between 150 and 220 K, which was attributed to the recovery of the single vacancy.

This absence of any 40 K stage in quenching experiments leads us to the natural conclusion that the 40 K stage that we observe in all cases is linked to the recovery of the interstitials; the simple 1 MeV behaviour is thought to be related to the fact that for this energy, just above the threshold energy of 0.7 MeV [1, 2], only close Frenkel pairs are created, so that at 40 K every interstitial falls back into the vacancy from which it comes; compare the 13 eV threshold energy value deduced in [2] with the maximum energy transfer value of 20.6 eV at 1 MeV, 38.6 eV at 1.5 MeV, and 89.8 eV at 2.5 MeV. We believe that the ideally simple result obtained for 1 MeV anneals is to be related to the large screening radius of the carriers in the semimetal Bi [10], which greatly favours the most simple process of vacancy–interstitial annihilation. On the contrary, at a higher irradiation energy such as 2.5 MeV, two mechanisms play a role; more complex defects are produced [2, 3], and the mean distance between interstitials and vacancies is larger. So, the 40 K recovery is not complete (some interstitials are 'lost' on surfaces, impurities or other defects or eventually agglomerate); a significant concentration of vacancies, not yet mobile at 40 K, remains. Thus we think that a significant number of defects remaining above 40 K are of the vacancy type; examination of the curves in figure 2 leads to the conclusion that above 40 K the recovery is more complete for the inverse of the electronic mobility than for the carrier density; this last fact, which is also evident in the Bi–Te and Bi–Sn alloys for which we studied the magnetotransport behaviour, is consistent with the donor character of the vacancy which we deduced in [2]. The 40 K stage presents a higher amplitude on the curves in figure 2 than on resistivity curves. A simple interpretation lies in the fact that $1/\bar{\mu}$ and $N-P$ vary in the same way so that the contributions of their variations to resistivity cancel approximately.

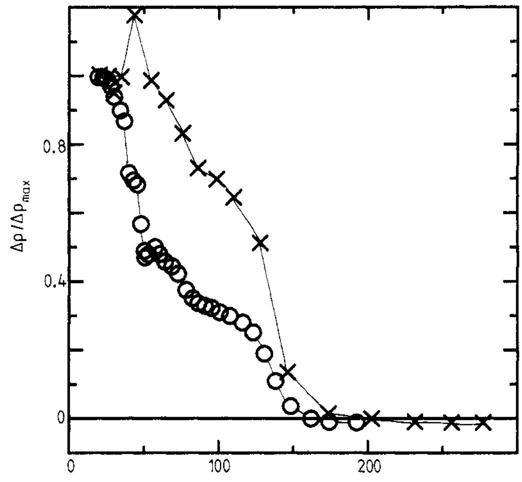

Figure 3. Isochronal annealing of resistivity after 1 MeV (high dose) and 1.5 MeV irradiations for two pure Bi samples: ○, sample Bi–D, 1.5 MeV; ×, sample Bi–E, 1 MeV.

In [9], positron lifetime measurements on some of our samples (pure Bi and dilute Bi–Te and Bi–Sn alloys) electron irradiated at 20 K and at 2.5 MeV and pre-annealed at 77 K are reported. From this technique, which has a preferential sensitivity to vacancy-like defects, it was concluded that long-range vacancy migration starts at 77 K in Bi. Because of the long 77 K anneal (several days), these measurements are quite preliminary. However, they seem to indicate that the monovacancy anneals in the small stage seen at around 80 K in figure 1, so that our larger stage near 140 K, together with the first stage in [4], would be related to the annealing of more complex vacancy-like defects (divacancies). Note that the vacancy clusters observed in [9] at 77 K disappear after annealing at 125 K, which is in agreement with the above statement.

3.3. *Other results*

Two complementary experiments were performed in which we measured the resistivity during annealing after first a long 1 MeV irradiation (corresponding to 2.6×10^{-3} dpa) and secondly a 1.5 MeV irradiation (5×10^{-3} dpa). The curves are reported in figure 3. In both cases the curves obtained look much like the 2.5 MeV curves in figure 1. At 1 MeV, only recombination can generate more complicated defects whereas, at 1.5 MeV, the computed cross section linked to complexes is only 12 b [1], to be compared to the value of 451 b for Frenkel pairs. From the value given in [3] for the recombination volume—between 100 and 200 atomic volumes—we see that the final doses for these two experiments are indeed in a regime where recombination plays an important role, so that a significant number of complex defects are present as for 2.5 MeV irradiations.

The 1 MeV sample of figure 3 shows a very peculiar behaviour: a 20% *increase* in resistivity after annealing near 40 K. We attribute this effect to electronic rather than metallurgical properties; from [2, 3] we know that, at 1 MeV, the number N of conduction electrons increases very rapidly on electron irradiation. This implies a maximum of resistivity in the production curve together with a low resistivity value at the end of the irradiation. Annealing has the opposite result; it decreases N and so possibly increases the resistivity.

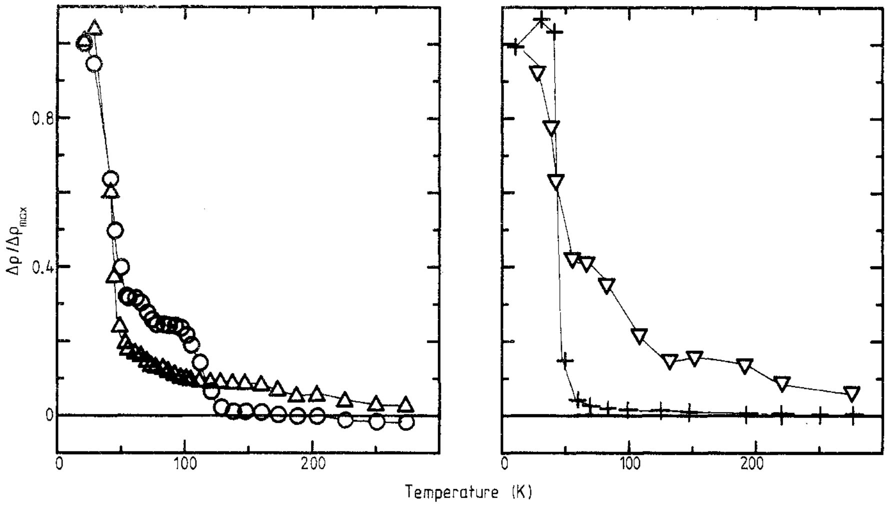

Figure 4. Isochronal annealing of resistivity after 2.5 MeV irradiations for Bi–Te and Bi–Sn samples: ○, sample Bi–Te–A; △, sample Bi–Sn–B; ▽, sample Bi–Sn–A; +, sample Bi–Sn–C.

We also need to discuss the influence of irradiation orientation because bismuth is known to be highly anisotropic. We found no difference between x-oriented and z-oriented samples, in the production curves (compare Bi I and Bi II in [3]) nor during the anneals (compare Bi-C and Bi-D in figure 1), irrespective of the energy. The conclusion is that there is no anisotropic effect in our experiments.

4. Bismuth-based dilute alloys

4.1. Introduction

It appeared wise to use dilute alloys as well as pure Bi samples, because impurities such as Sn (donor) or Te (acceptor) have doping properties, which implies that one can scan the band structure by doping, as established in [11]. In [3], we showed the existence of a virtual bound state in the band structure, situated slightly below the intrinsic (pure Bi) Fermi level, linked to the defect complexes. This implies that it would be very interesting to investigate the behaviour of samples with low-lying Fermi levels, i.e. Bi–Sn samples containing more than 50 at.ppm Sn. The samples are described in table 1.

4.2. 1 and 2.5 MeV irradiations: annealing results

We shall not describe 1 MeV irradiations performed on other samples [1] here; the net result is that one single stage appears at the same temperature as in pure Bi. The results concerning dilute alloys when irradiated at 2.5 MeV are reported in figure 4. The most important fact is that the temperatures at which the different stages occur are nearly the same as in pure Bi. The main differences from the Bi case are as follows.

(i) The amplitudes of the stages are different (the 40 K stage seems to be always more complete in terms of resistance annealing in the alloys).

(ii) A constant behaviour specific to Bi–Te samples is that the resistivity after room temperature annealing is always lower than before irradiation; from magnetotransport data it appears that this corresponds to both a lower-lying Fermi level and a higher mobility.

4.3. Discussion

Here we propose only qualitative ideas concerning the comparison between pure Bi and dilute alloys. We group the samples into two classes.

(i) The high-Fermi-level sample group consists of pure Bi, Bi–Te and Bi–Sn with less than 50 at.ppm Sn content. For these samples the annealing curves are seen to be very similar. The curve for sample Bi–Te-A is somewhat lower; this can be related to the much more linear character of the production curve as described in [3], leading to a lower resistivity weight placed on small defect concentrations and thus enlarging the relative amplitude of the first stage. On the contrary, the stages occur at the same temperatures for each case, from which we conclude that only the difference betwen these samples is the different electronic properties of the carriers. The only exception is the final (i.e. after a complete anneal) resistivity of Bi–Te samples, which is always lower than the initial resistivity. The Fermi level is lower, and the mobility is higher; both indicate some loss of tellurium, corresponding possibly to the Te–interstitial interaction found in [9].

(ii) The low-Fermi-level sample group comprises solely Bi–Sn with more than 50 at.ppm Sn content. For these samples the annealing curves are much lower, looking like the 1 MeV curves for a high Sn content. In particular, the 140 K stage seems to have disappeared for these Sn-concentrated samples, Here again, the properties of free carriers can account for this predominancy of the 40 K stage. During the anneals the Fermi level crosses the virtual bound level studied in [3], which can be expressed in terms of mean electric charge of one defect; this charge is then thought to increase from typically 0.03 to 0.18 during anneals and most probably during the 40 K stage. The net consequence is that the mobilities must anneal much more completely than $N - P$ during this stage, leading to a very important resistivity reduction as observed. (As mentioned in [3], an analysis of the magnetotransport measurements for sample Bi–Sn-C was impossible and so no direct check of these ideas was possible.) However, we are not able at present to state without ambiguity that the disappearance of the 140 K stage is due only to such electronic properties and not to Sn–defect interaction. The results in [9] corroborate such an interaction; in [9] the formation of stable vacancy–Sn complexes was seen, preventing the formation of divacancies and so preventing the existence of a stage at 140 K.

5. Conclusion

The most spectacular result of our work lies in the 1 MeV annealing curves: a single-stage anneal, which is an ideally simple and very rare case. This stage is attributed to the complete annihilation of each Frankel pair as a consequence of the interstitial migration. This seems to be confirmed by higher-energy results where vacancies remain after this stage. We attribute the stages seen at 2.5 MeV to the migration of vacancies (near 80 K) and possibly divacancies (near 130 K). We also prove that in our dilute alloys samples the effect of defect–impurity interaction on transport properties is quite small; in these samples, the annealing properties are dominated by effects coming from the variation in the number of carriers with the concentration of defects. Defect–impurity interactions can only be unambiguously shown by more vacancy-sensitive experiments such as positron lifetime measurements, which reveal Sn–vacancy and Te–interstitial interactions. The Te–interstitial interaction can be thought to be responsible for the 'loss' of Te found in § 4.2, whereas the Sn–vacancy interaction is a possible explanation for the lack of a 140 K stage in the annealing curves of the more concentrated Bi–Sn alloys.

Acknowledgment

Numerous discussions with D Lesueur are gratefully acknowledged.

References

[1] Bois P 1986 *Thesis* Université d'Orsay; Report CEA-R-5389
[2] Bois P and Beuneu F 1987 *J. Phys. F: Met. Phys.* **17** 2365
[3] Beuneu F and Bois P 1988 *Phys. Rev.* B **37** 6041
[4] Bittar A and Lesueur D 1978 *Phys. Status Solidi* a **48** K123
[5] Quélard G and Lesueur D 1976 *Phys. Status Solidi* a **36** 729
[6] Quélard G 1977 *Thesis* Université de Nancy; Report CEA-R-4866
[7] Weck W, Gerstenberg H and Müller P 1984 *Proc. 17th Low Temperature Conf. (Karlsruhe)* (Amsterdam: North-Holland) p 1383
[8] Le Goff M 1984 *Thesis* Université Paris-Nord; Report CEA-R-5288
[9] Corbel C, Bois P, Moser P and Lemahieu I 1986 *Int. Conf. Vacancies and Interstitials in Metals and Alloys (Berlin) 1987; Mater. Sci. Forum* **15–18** 721
[10] Brownell D H and Hygh E H 1967 *Phys. Rev.* **164** 909
[11] Noothoven van Goor J M 1971 *Philips Res. Rep. Suppl.* **4** 1